

Laser Photolysis of Iron(III) Tetraphenylporphyrin in Methanol. A Kinetic Study on the Formation of the Superoxide Anion Radical from the Dioxygen Adduct of Iron(II) Tetraphenylporphyrin

Mikio Hoshino* and Tomoya Baba

The Institute of Physical and Chemical Research
Wako, Saitama 351, Japan

Received March 2, 1998

Chemical reactions of synthetic iron(II) porphyrins and dioxygen have attracted much attention because of their importance as model systems for understanding the roles and functions of natural hemoproteins in vivo.^{1–9} Earlier studies of these reactions have mainly focused on the reversible binding of dioxygen by iron(II) porphyrins,^{10–15} and less attention has been paid to the formation of O₂^{•-} from the reaction of synthetic iron(II) porphyrins and dioxygen.

In 1933, neutrophils were found to exhibit a “respiratory burst” upon exposure to certain stimuli, producing the potentially microbicidal reagent, O₂^{•-}.^{16,17} Subsequent studies revealed that the O₂^{•-} producing enzyme in neutrophils contains the heme-protein, cytochrome *b*₅₅₈, which plays an essential role in the catalytic reduction of dioxygen at the expense of NADPH.^{17–27} The formation of O₂^{•-} has also been observed in the autoxidation processes of ferro-myoglobin and -hemoglobin, which, although

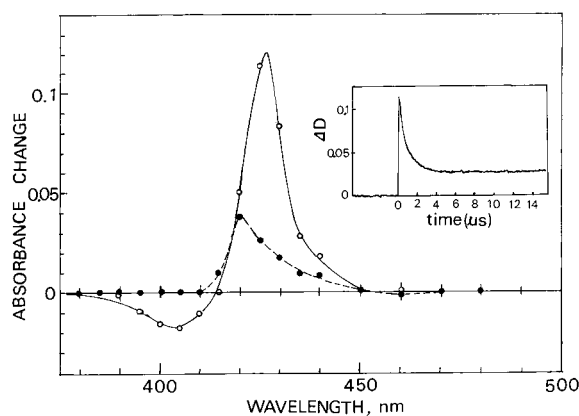


Figure 1. Transient absorption spectra observed for the methanol solution of 1.0×10^{-5} M ClFe^{III}TPP saturated with oxygen gas at 1 atm, at 50 ns (open circle) and 10 μ s (closed circle) after the 355-nm laser pulse. The decay of the transient monitored at 425 nm is shown in the inset.

slowly, reduce dioxygen to yield O₂^{•-}.^{28–30} Thus, studies on the O₂^{•-} production by iron(II) porphyrins are important for elucidation of the reduction mechanism of dioxygen by ferro-hemoproteins in vivo. The present kinetic study demonstrates that Fe^{II}TPP (TPP = tetraphenylporphyrin) produced by laser photolysis of ClFe^{III}TPP in methanol reacts with dioxygen to give the dioxygen adduct, (O₂)Fe^{II}TPP, which dissociates O₂^{•-} to regenerate Fe^{III}TPP⁺.

Continuous photolysis of ClFe^{III}TPP in methanol was carried out by a 250 W mercury lamp with a cutoff filter ($\lambda > 330$ nm). In the aerated methanol solution, ClFe^{III}TPP was slightly photo-decomposed. However, the degassed methanol solution quantitatively yields (CH₃OH)₂Fe^{II}TPP upon irradiation.³¹

The spectrum of (CH₃OH)₂Fe^{II}TPP in methanol exhibits an absorption peak at 425 nm ($\epsilon = 2.26 \times 10^5$ M⁻¹ cm⁻¹). When the methanol solution was exposed to air, the spectrum of (CH₃OH)₂Fe^{II}TPP instantaneously returned to that of ClFe^{III}TPP in methanol measured before irradiation.

The photochemical formation of Fe^{II}TPP was again confirmed by the 355-nm laser photolysis of ClFe^{III}TPP in degassed methanol, i.e., the transient spectrum measured at 50 ns after the pulse has a positive peak at 425 nm and a negative one at 405 nm, in good agreement with the difference spectrum (Fe^{II}TPP minus ClFe^{III}TPP). The quantum yield for the formation of Fe^{II}TPP is ca. 0.02. Fe^{II}TPP produced in degassed methanol was found to exhibit neither a decay nor a rise over a few milliseconds after the laser pulse.

Figure 1 shows the transient absorption spectra observed for an oxygen-saturated methanol solution of 1.0×10^{-5} M ClFe^{III}TPP at 50 ns and 10 μ s delay after a 355-nm laser pulse. The 50-ns spectrum is identical with that observed for the degassed methanol solution, indicating the formation of Fe^{II}TPP. The decay of Fe^{II}TPP in oxygen-saturated methanol was investigated by monitoring the absorbance change at 425 nm. As shown in the inset of Figure 1, the absorbance change, ΔD , at 425 nm decreases with time and levels off within several microseconds after the laser pulse. This result is best interpreted in terms of the reaction of Fe^{II}TPP and O₂, i.e., the Fe^{II}TPP reacts with oxygen to produce the dioxygen adduct of Fe^{II}TPP,

(1) James, B. R. In *The Porphyrins*; Dolphin, D., Ed.; Academic Press: New York, 1978; Vol. V, Chapter 6.

(2) Collman, J. P.; Brauman, J. I.; Iverson, B. Z.; Sessler, J. L.; Morris, R. M.; Gibson, Q. H. *J. Am. Chem. Soc.* **1983**, *105*, 3052–3064 and references therein.

(3) Chang, C. K.; Traylor, T. G. *Proc. Natl. Acad. Sci. U.S.A.* **1973**, *70*, 2647–2650.

(4) Olafson, B. D.; Goddard, W. A., III *Proc. Natl. Acad. Sci. U.S.A.* **1977**, *74*, 1315–1319.

(5) Chang, C. K.; Traylor, T. G. *Proc. Natl. Acad. Sci. U.S.A.* **1975**, *72*, 1160–1170.

(6) Collman, J. P. *Acc. Chem. Res.* **1977**, *10*, 265–271.

(7) Weschler, C. J.; Anderson, D. L.; Basolo, F. *J. Am. Chem. Soc.* **1975**, *97*, 6707–6712.

(8) Cohen, I. A.; Caughey, W. S. *Biochemistry* **1968**, *7*, 636–641.

(9) Reed, C. A.; Cheung, S. K. *Proc. Natl. Acad. Sci. U.S.A.* **1977**, *74*, 1780–1784.

(10) Alben, J. O.; Fuchsman, W. H.; Beaudreau, C. A.; Caughey, W. S. *Biochemistry* **1968**, *7*, 624–635.

(11) Wagner, G. C.; Kessner, R. J. *J. Am. Chem. Soc.* **1974**, *96*, 5593–5595.

(12) Brinigar, W. S.; Chang, C. K. *J. Am. Chem. Soc.* **1974**, *96*, 5595–5597.

(13) Brinigar, W. S.; Chang, C. K.; Geibel, J.; Traylor, T. G. *J. Am. Chem. Soc.* **1974**, *96*, 5597–5599.

(14) Anderson, D. L.; Weschler, C. J.; Basolo, F. *J. Am. Chem. Soc.* **1974**, *96*, 5599–5600.

(15) Almog, J. A.; Baldwin, J. E.; Dyer, R. L.; Huff, J.; Wilkerson, C. J. *J. Am. Chem. Soc.* **1974**, *96*, 5600–5601.

(16) Baldrige, C. W.; Gerrard, R. W. *Am. J. Physiol.* **1933**, *103*, 235–236.

(17) Cross, A. R.; Jones, O. T. G. *Biochem. Biophys. Acta* **1991**, *1057*, 281–298.

(18) Segal, A. W. *Biochem. Soc. Trans.* **1989**, *17*, 427–434.

(19) Segal, A. W. *Nature* **1987**, *326*, 88–91.

(20) Cross, A. R. *Biochem. Pharmacol.* **1987**, *36*, 489–493.

(21) Rapoport, R.; Hamukoglu, I.; Sklan, D. *Anal. Biochem.* **1994**, *218*, 309–313.

(22) Doussiere, J.; Vignais, P. V. *Biochem. Biophys. Res. Commun.* **1991**, *175*, 143–151.

(23) Isogai, Y.; Iizuka, T.; Makino, R.; Iyanagi, T.; Orii, Y. *J. Biol. Chem.* **1993**, *268*, 4025–4013.

(24) Foroozan, R.; Ruedi, J. M.; Babior, B. M. *J. Biol. Chem.* **1992**, *267*, 24400–24407.

(25) Koshkin, V.; Picke, E. *FEBS Lett.* **1994**, *338*, 285–289.

(26) Kramer, D. M.; Crofts, A. R. *Biochim. Biophys. Acta* **1994**, *11284*, 193–201.

(27) Morel, F.; Doussiere, J.; Stasia, M.-J.; Vignais, P. V. *Eur. J. Biochem.* **1985**, *152*, 669–679.

(28) Springer, B. A.; Egeberg, K. D.; Sliagar, S. G.; Rohlfes, R. J.; Mathews, A. J.; Olson, J. S. *J. Biol. Chem.* **1989**, *264*, 3057–3060.

(29) Brantley, R. E., Jr.; Smerdon, S. J.; Wilkinson, A. J.; Singleton, E. W.; Olson, J. S. *J. Biol. Chem.* **1993**, *268*, 6995–7010.

(30) Shiro, Y.; Iwata, T.; Makino, R.; Fujii, M.; Isogai, Y.; Iizuka, T. *J. Biol. Chem.* **1993**, *268*, 19983–19990.

(31) Hoshino, M.; Ueda, K.; Takahashi, M.; Yamaji, Y.; Hama, Y. *J. Chem. Soc., Faraday Trans.* **1992**, *88*, 405–408.

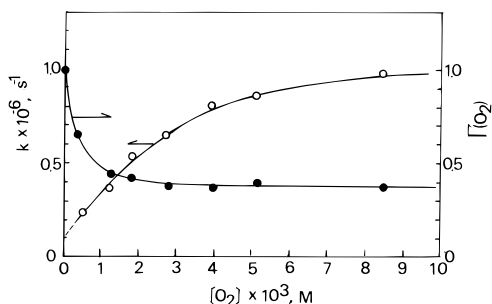


Figure 2. The plots of the decay rate constants (open circle), k , and the $\Gamma(\text{O}_2)$ values (closed circle) represented as a function of the oxygen concentration (see text). The solid curves of k and $\Gamma(\text{O}_2)$ are, respectively, calculated with the use of eqs 8 and 10: parameters used are $k_f = 1.25 \times 10^6 \text{ s}^{-1}$, $k_d = 1.0 \times 10^5 \text{ s}^{-1}$, and $k_c/k_b = 3.6 \times 10^2 \text{ M}^{-1}$ for k and $\gamma = 0.35$ and $K = 4.5 \times 10^3 \text{ M}^{-1}$ for $\Gamma(\text{O}_2)$.

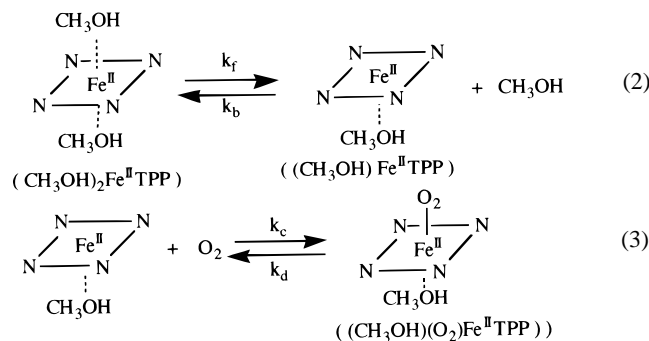
$(\text{CH}_3\text{OH})(\text{O}_2)\text{Fe}^{\text{II}}\text{TPP}$, which gives the 10- μs spectrum. The 10- μs spectrum having a positive peak at 420 nm eventually disappeared according to first-order kinetics over a few hundred milliseconds after the pulse: the rate constant is 14 s^{-1} .

The decay of the absorbance change, ΔD , at 425 nm is expressed by

$$\Delta D = \Delta D_0 \exp(-kt) + \Delta D_\infty \quad (1)$$

The plot of $\ln(\Delta D - \Delta D_\infty)$ vs t gives a straight line with a slope k . The rate constants, k , were measured as a function of the oxygen concentration, $[\text{O}_2]$.

Figure 2 shows the plot of k vs $[\text{O}_2]$. The value of k asymptotically approaches to a limiting value with an increase in $[\text{O}_2]$. We, therefore, consider that the dioxygen adduct, $(\text{CH}_3\text{OH})(\text{O}_2)\text{Fe}^{\text{II}}\text{TPP}$, is produced according to the following reaction mechanism.



When the steady-state approximation is taken with regard to $(\text{CH}_3\text{OH})\text{Fe}^{\text{II}}\text{TPP}$, the rate constant, k , for the decay of $(\text{CH}_3\text{OH})_2\text{Fe}^{\text{II}}\text{TPP}$ is formulated as

$$k = \frac{k_f k_c [\text{O}_2] + k_b k_d}{k_b + k_c [\text{O}_2]} \quad (4)$$

The plot of k vs $[\text{O}_2]$ in Figure 2 gives $k_f = 1.25 \times 10^6 \text{ s}^{-1}$, $k_d = 1.0 \times 10^5 \text{ s}^{-1}$, and $k_c/k_b = 3.6 \times 10^2 \text{ M}^{-1}$. The equilibrium constant, K , for the formation of $(\text{CH}_3\text{OH})(\text{O}_2)\text{Fe}^{\text{II}}\text{TPP}$ in methanol is given by

$$K = k_f k_c / k_b k_d = 4.5 \times 10^3 \text{ M}^{-1} \quad (5)$$

This value is in moderate agreement with those obtained for the formation of the dioxygen adducts of manganese(II) tetraphenylporphyrin³² and iron(II) picket fence porphyrins² in toluene solutions.

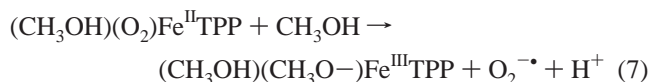
The formation mechanism of the dioxygen adduct described above is again supported kinetically. From eq 1, the initial absorbance change, $\Delta D(t=0)$, is expressed as $\Delta D(t=0) = \Delta D_0 + \Delta D_\infty$. The ratio, $\Gamma(\text{O}_2) = \Delta D_\infty / \Delta D(t=0)$, is a function of the oxygen concentration. Equations 2 and 3 give an expression for $\Gamma(\text{O}_2)$, i.e.,

$$\Gamma(\text{O}_2) = (1 + \gamma K [\text{O}_2]) / (1 + K [\text{O}_2]) \quad (6)$$

where γ is the value of $\Gamma(\text{O}_2)$ at an “infinite” concentration of oxygen.

As shown in Figure 2, the value of $\Gamma(\text{O}_2)$ measured in the range $0 < [\text{O}_2] < 8.5 \times 10^{-3} \text{ M}$ decreases with an increase in $[\text{O}_2]$ to attain a constant value at the oxygen concentration higher than ca. $4 \times 10^{-3} \text{ M}$. The plot of $\Gamma(\text{O}_2)$ vs $[\text{O}_2]$ is well reproduced by eq 6 with the use of $\gamma = 0.35$ and $K = 4.5 \times 10^3 \text{ M}^{-1}$. The fact that the equilibrium constant obtained from eq 6 is identical with that from eq 5 supports the mechanism of the reversible formation of $(\text{CH}_3\text{OH})(\text{O}_2)\text{Fe}^{\text{II}}\text{TPP}$ mentioned above.

Continuous photolysis of $\text{ClFe}^{\text{III}}\text{TPP}$ in methanol reveals that $(\text{CH}_3\text{OH})_2\text{Fe}^{\text{III}}\text{TPP}$ reacts with oxygen and eventually returns to the iron(III) porphyrin. This result suggests that the dissociation of $\text{O}_2^{\cdot -}$ occurs from $(\text{O}_2)\text{Fe}^{\text{II}}\text{TPP}$.



Detection of $\text{O}_2^{\cdot -}$ produced by autodissociation from the dioxygen adduct, $(\text{CH}_3\text{OH})(\text{O}_2)\text{Fe}^{\text{II}}\text{TPP}$, was made by the spin trapping method. The aerated methanol solution of $1.0 \times 10^{-5} \text{ M}$ $(\text{Cl})\text{Fe}^{\text{III}}\text{TPP}$ and $1.0 \times 10^{-2} \text{ M}$ DMPO (5,5'-dimethyl-1-pyrroline *N*-oxide) was irradiated by the mercury lamp with the cutoff filter ($\lambda > 330 \text{ nm}$). The ESR spectrum of the DMPO adduct thus obtained exhibits $A_N = 13.5 \pm 0.3$ and $A_H^\alpha = 10.0 \pm 0.3$, in good agreement with those reported for the $\text{O}_2^{\cdot -}$ (or $\text{HO}\cdot$) adduct of DMPO in methanol.³³

The laser photolysis studies of $\text{ClFe}^{\text{III}}\text{TPP}$ in oxygen-saturated methanol revealed that the dioxygen adduct, $(\text{CH}_3\text{OH})(\text{O}_2)\text{Fe}^{\text{II}}\text{TPP}$, slowly decays with the first-order rate constant of 14 s^{-1} . The rate constant was found to be almost independent of $[\text{O}_2]$ in the concentration range $[\text{O}_2] > 1.0 \times 10^{-3} \text{ M}$. This finding implies that the rate for the dissociation of $\text{O}_2^{\cdot -}$ is much slower than that for achieving the equilibrium shown by eqs 4 and 5. The rate constant is four or five orders of magnitude larger than those measured for the dioxygen adducts of native, mutant, and tetrazorium-modified myoglobins in aqueous solution.^{28–30,34}

An outer-sphere electron-transfer reaction from reduced hemes to dioxygen has been assumed for the oxidation of cytochrome b_{558} .³⁵ The oxidation mechanism of myoglobin by dioxygen has been explained by a combination of an outer-sphere electron-transfer reaction from myoglobin to dioxygen and a unimolecular ionic dissociation of $\text{O}_2^{\cdot -}$ from oxymyoglobin.^{29,34} In the present study, we conclude that the outer-sphere electron transfer does not take place from both $(\text{CH}_3\text{OH})_2\text{Fe}^{\text{II}}\text{TPP}$ and $(\text{CH}_3\text{OH})\text{Fe}^{\text{II}}\text{TPP}$ to dioxygen because of the facts that (1) the rate constant k increases and asymptotically levels off with an increase in $[\text{O}_2]$ and (2), unlike the oxidation of myoglobin, the rate constant k does not exhibit a “bell-shaped” O_2 concentration dependence.²⁹

Further studies are in progress.

JA9806783

(33) Harbor, J. R.; Hair, M. L. *J. Phys. Chem.* **1978**, *82*, 1397–1399.

(34) Wallace, W. J.; Houtchens, R. A.; Maxwell, J. C.; Caughey, W. S. *J. Biol. Chem.* **1982**, *257*, 4966–4977.

(35) Isogai, Y.; Iizuka, T.; Shiro, Y. *J. Biol. Chem.* **1995**, *270*, 7853–7857.